High-Resolution X-Ray Spectroscopy of Supernova Remnants: From Dispersive Spectrometer to Micro-calorimeter

Satoru Katsuda (Saitama University, Japan)

Need for High-Res. X-Ray Spectroscopy

Scientific motivations

- SN explosion physics
- Progenitors
- SN nucleosynthesis
- Chemical evolution of galaxies

- Collisionless shock physics
- Particle acceleration

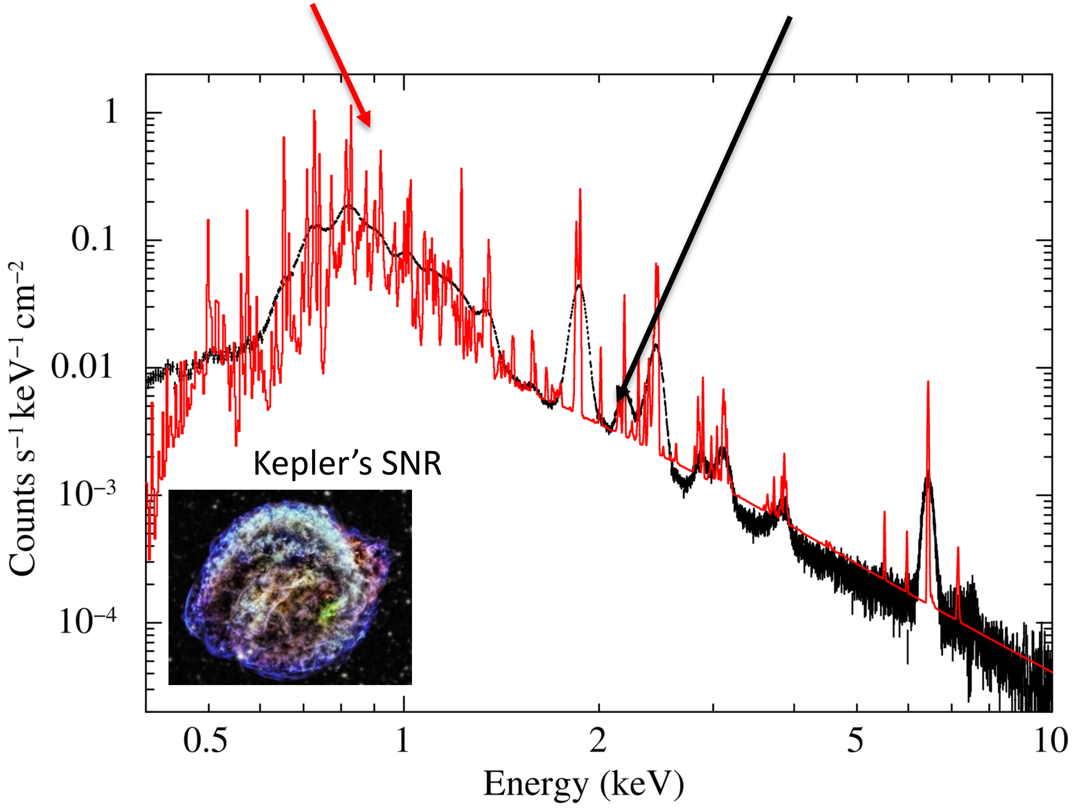
Theoretical model vs. Data with Suzaku XIS (E/ΔE ~ 20)

X-ray CCDs can not resolve fine structures.
→ Better resolution (E/ΔE > 100) is a must!

Micro-calorimeter (Resolve) aboard XRISM

After three Japan-US led missions ASTRO-E1 (2000), Suzaku (2005-2015), Hitomi (2016), we finally have an in-orbit X-ray microcalorimeter since 2023!

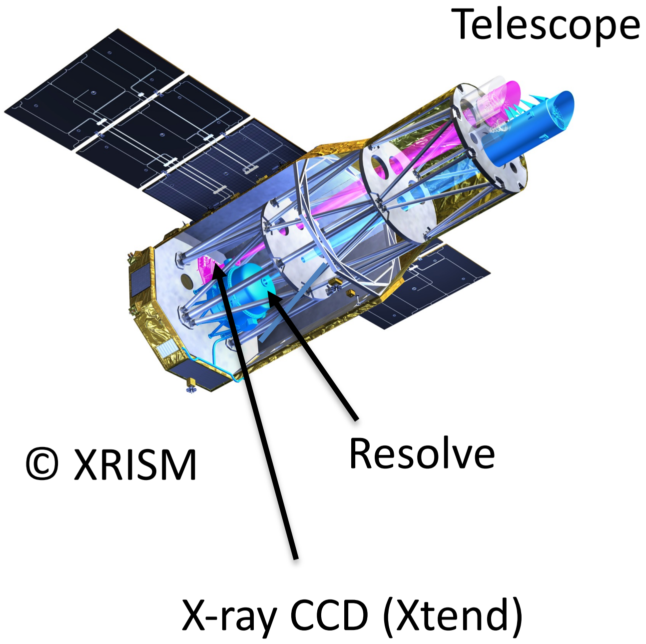

© XRISM

☐ XRISM:

- The 7th Japanese X-ray astronomy satellite
- Successfully launched on Sep. 7th 2023

☐ X-ray micro-calorimeter (Resolve):

- ΔE: ~5 eV (Non-dispersive!)
- Spatial resolution: ~1’
- FoV: 3’x3’ (6x6 array)
- Dynamic range: 0.2-10 keV
  (NB: 2-10 keV at this moment)

Some early results were presented in this conference by B. Williams and P. Plucinsky.

Gratings onboard XMM-Newton & Chandra

XMM-Newton's RGS

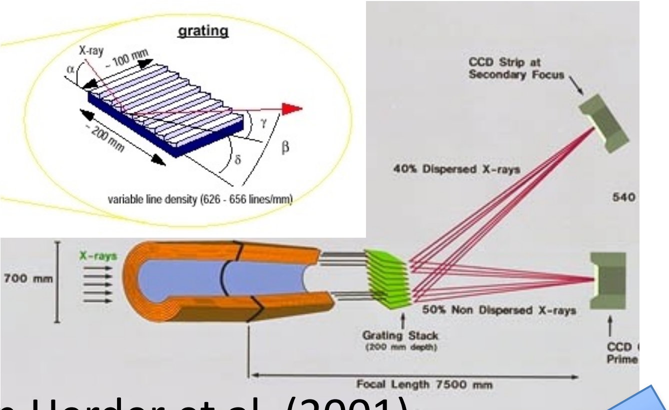

den Herder et al. (2001)

Chandra's HETG&LETG

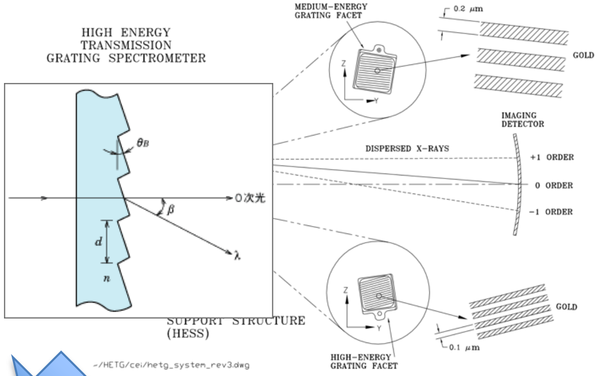

Canizares et al. (2005)

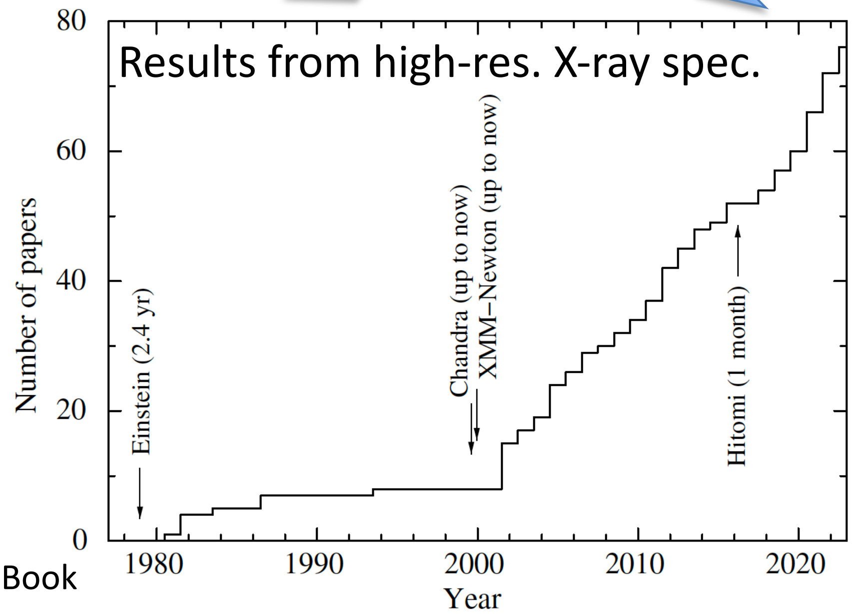

SK (2023) Springer Book

In case of Resolve's gate-valve closed, the gratings and Resolve are complementary in terms of the energy coverage.

Gratings onboard XMM-Newton & Chandra

Spectral resolution of a grating spectrometer:

$\Delta\lambda \sim d \sin\alpha \, \Delta\theta / m$

d: grating spacing (Å)

α: angle of incidence

$\Delta\theta$: spatial extent of the source or telescope's angular resolution for a point source

m: spectral order

	Chandra HEG	**Chandra MEG**	**XMM RGS**
d (Å)	2000	4000	15500
α	~90 deg	~90 deg	~1.6 deg
d sin α (Å)	2000	4000	420
$\Delta\lambda$ (Å for m=1; $\Delta\theta$ = PSF)	0.01	0.02	0.03
$\Delta\lambda$ (Å for m=1; $\Delta\theta$ = 1')	0.58	1.16	0.12

Strong for ″-scale sources

Strong for ′-scale sources

Specific Sciences from High-Res. Spectroscopy

- Ejecta dynamics
  - 3D ejecta/CSM structures
- Collisionless shock physics
  - T_i-T_e equilibration
  - Cosmic-ray acceleration
- Plasma diagnostics
  - New emission processes
  - Thermodynamic parameters
- Composition measurements
  - Odd-Z/neutron-rich elements

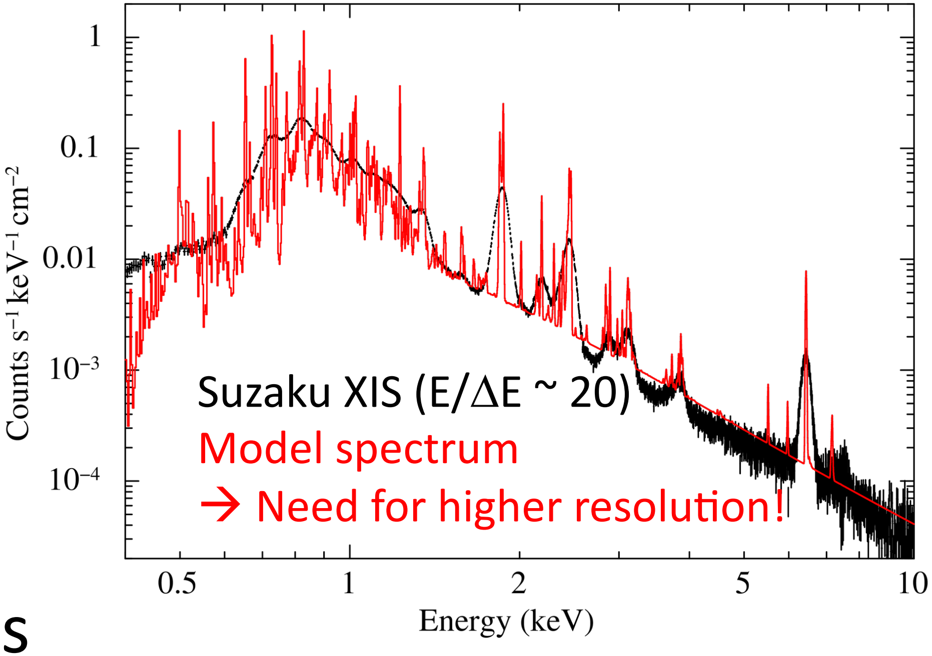

Suzaku XIS (E/ΔE ~ 20)

Model spectrum

→ Need for higher resolution!

3D Structures of Young SNRs

3D ejecta distributions are the key to understand the progenitor and explosion mechanism.

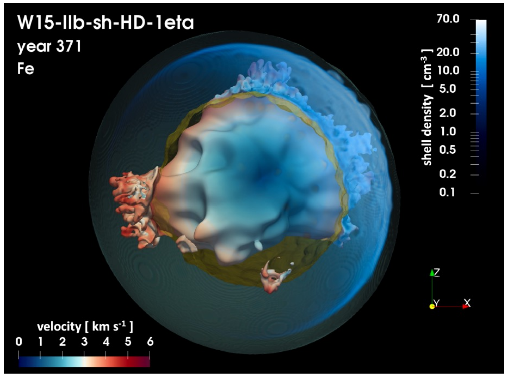

3D hydrodynamic simulation
(e.g., Orlando et al. 2022)

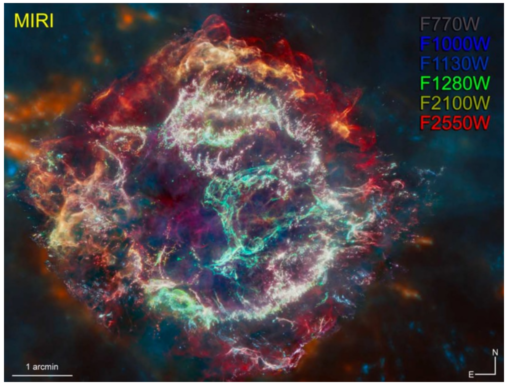

JWST view (e.g., Milisavljevic et al. 2024)

- Si-rich jets
→ jet-induced explosion
- Fe/Si inversion, Ti-rich ejecta
→ high-entropy ejecta plume
- Ni bubble effects

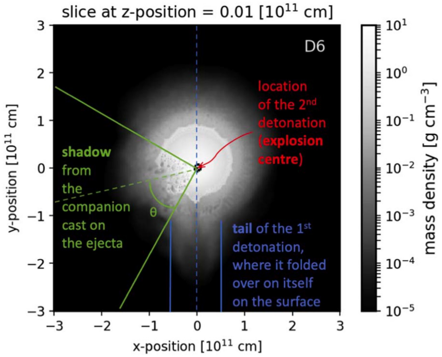

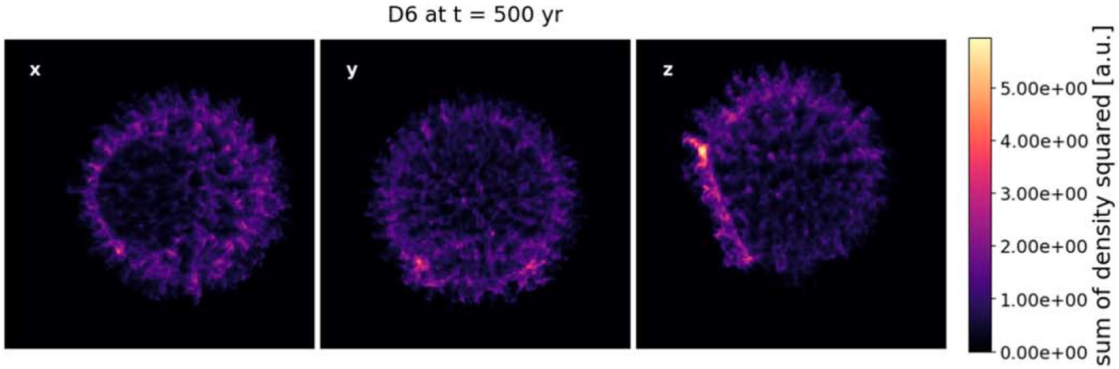

Remnant of Type Ia D6 model (Ferrand et al. 2022)

Cas A with Chandra/HETG

HETG spectroscopy (Lazendic et al. 2006)

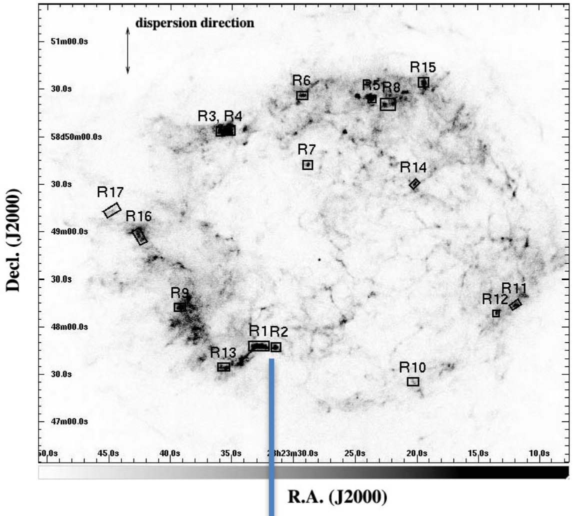

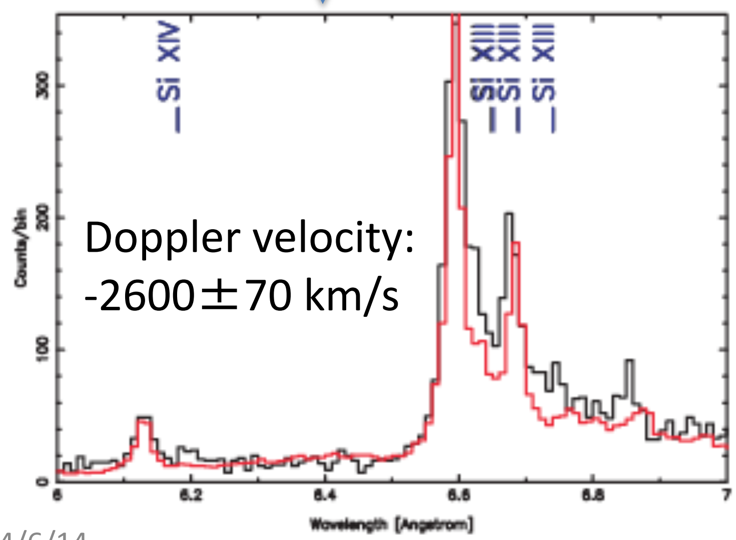

Doppler velocity:
-2600±70 km/s

Line of sight locations of 21 knots measured by Si K lines

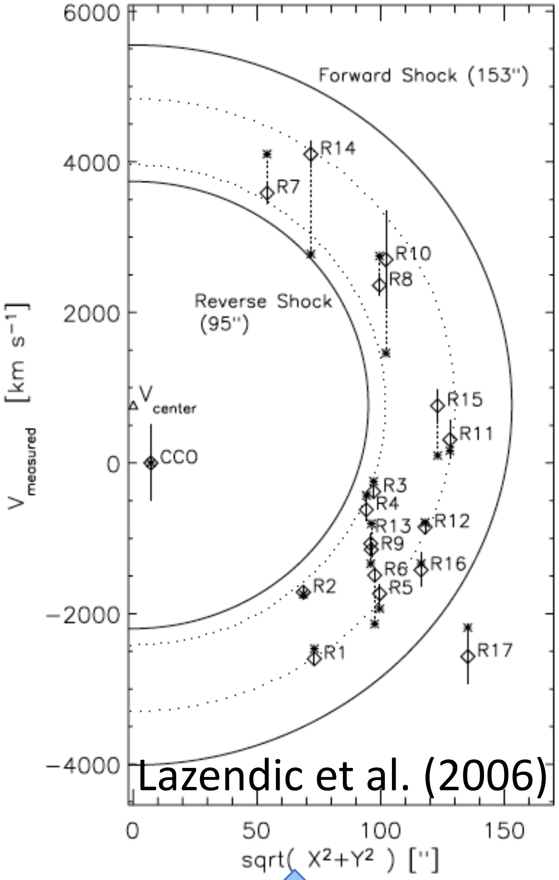

Lazendic et al. (2006)

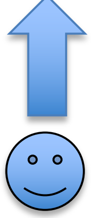

Line of sight

G292.0+1.8 with Chandra/HETG

HETG spectroscopy (Bhalerao et al. 2015)

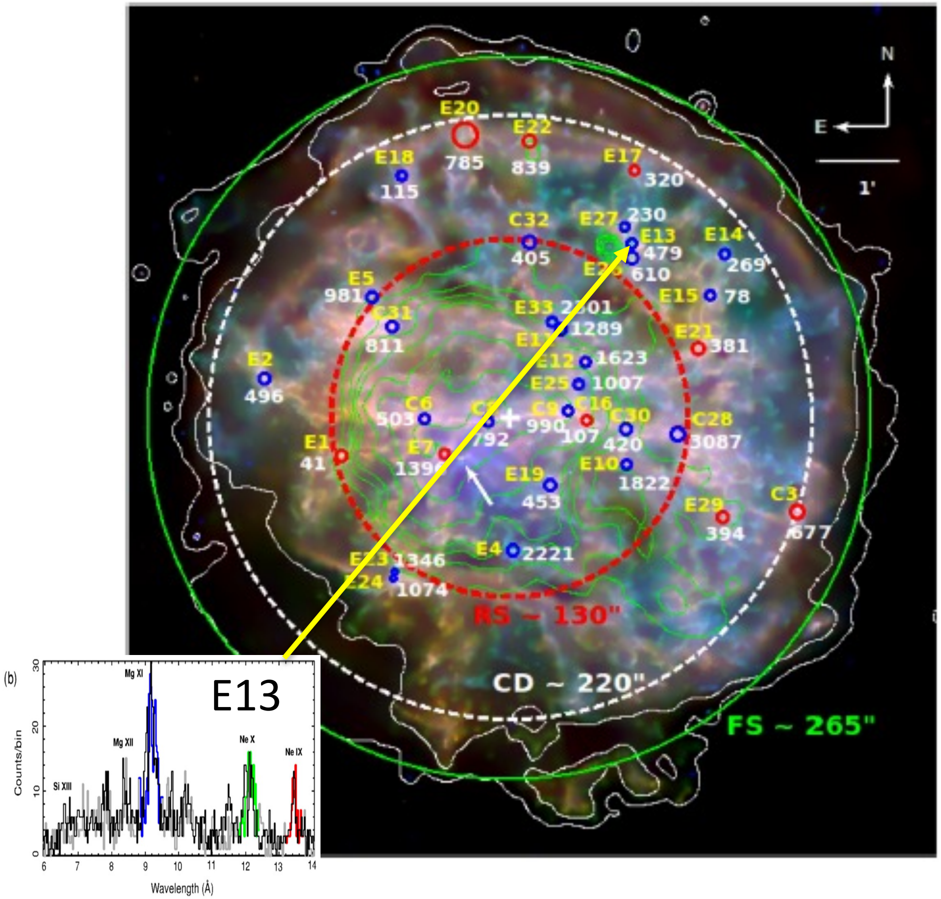

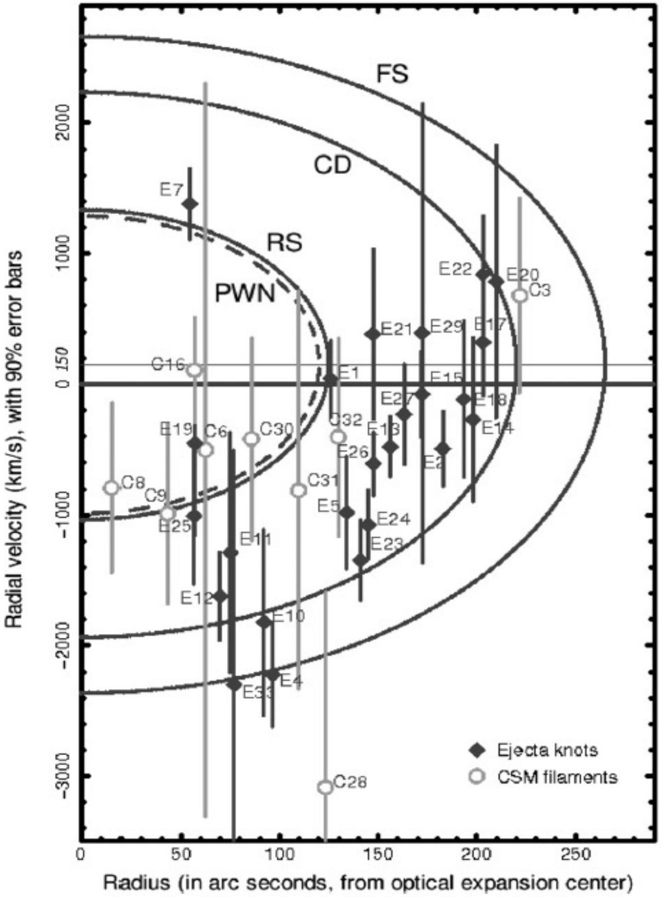

☐ More ejecta reside in the near side. → Asymmetric explosion?

☐ The ejecta distribution suggests $R_{RS}/R_{FS} \sim 0.5$.

Puppis A: ONeMg-rich Ejecta

RGS spectroscopy of the ejecta features (SK+2013)

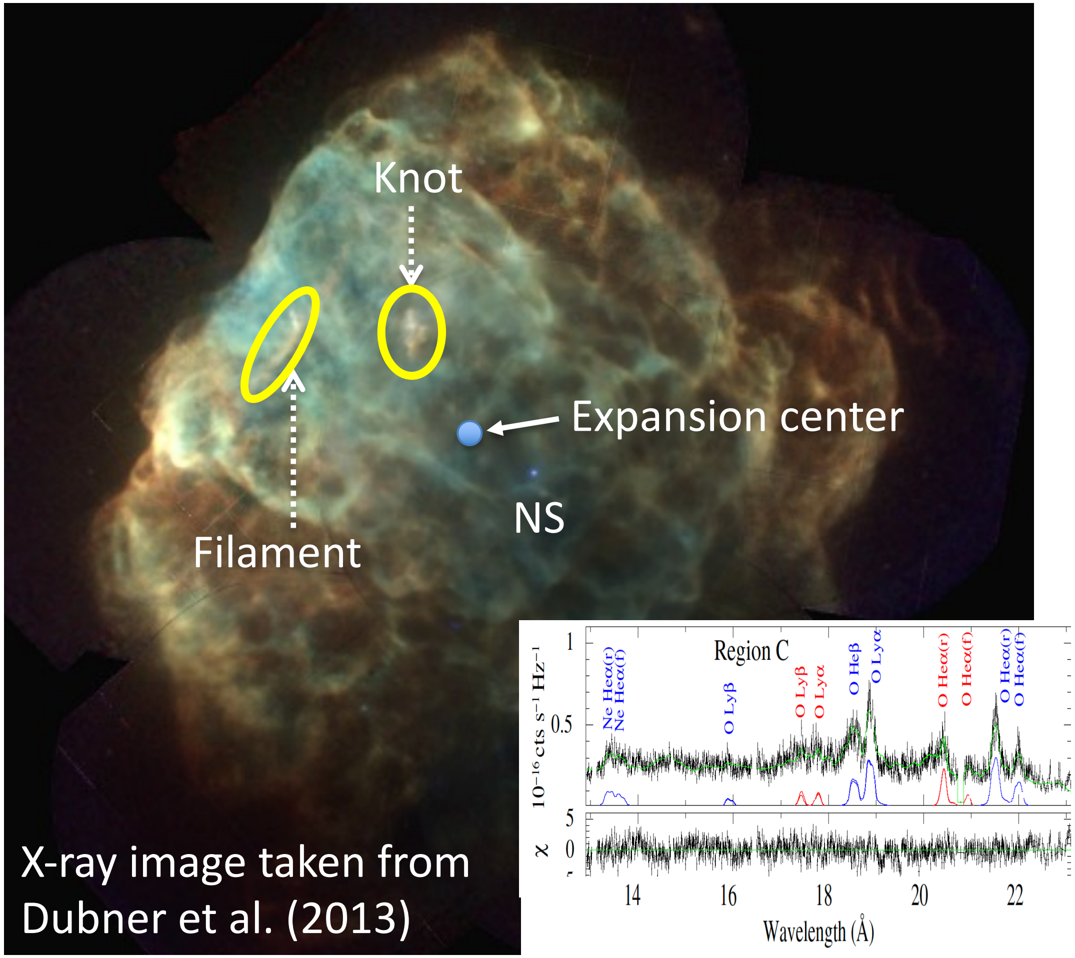

X-ray image taken from Dubner et al. (2013)

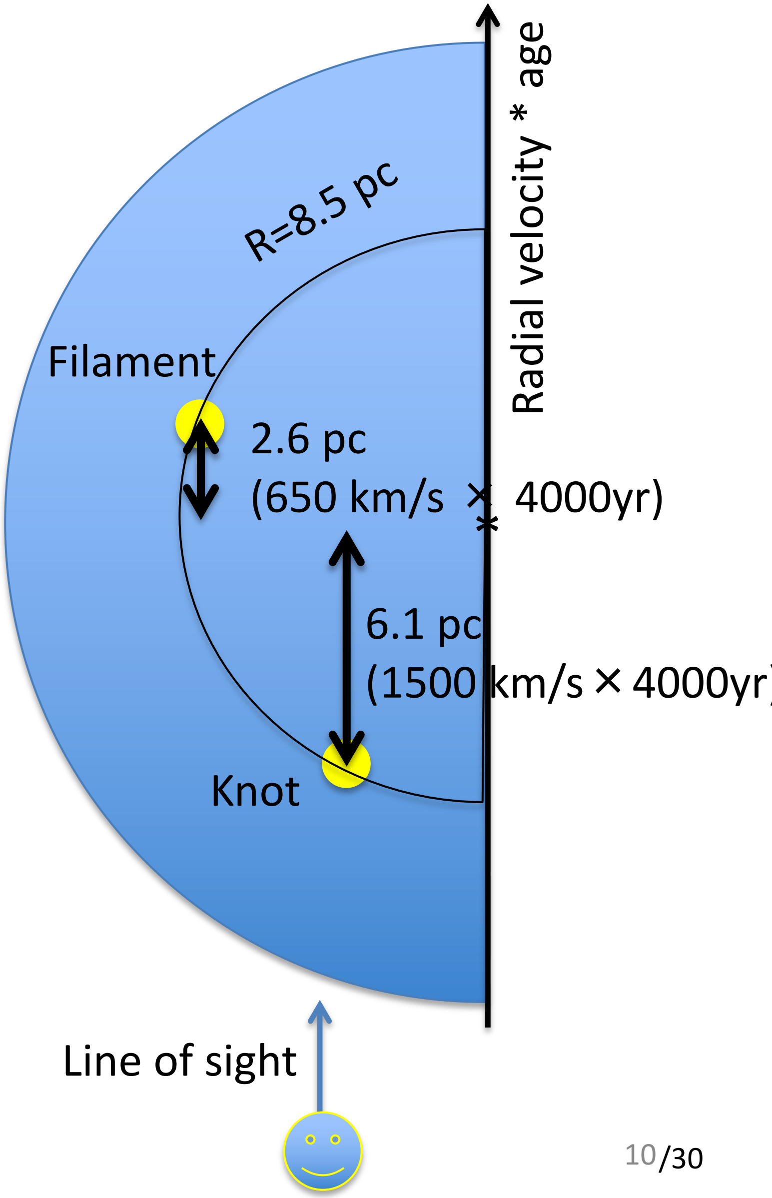

Puppis A: Fe-rich Ejecta

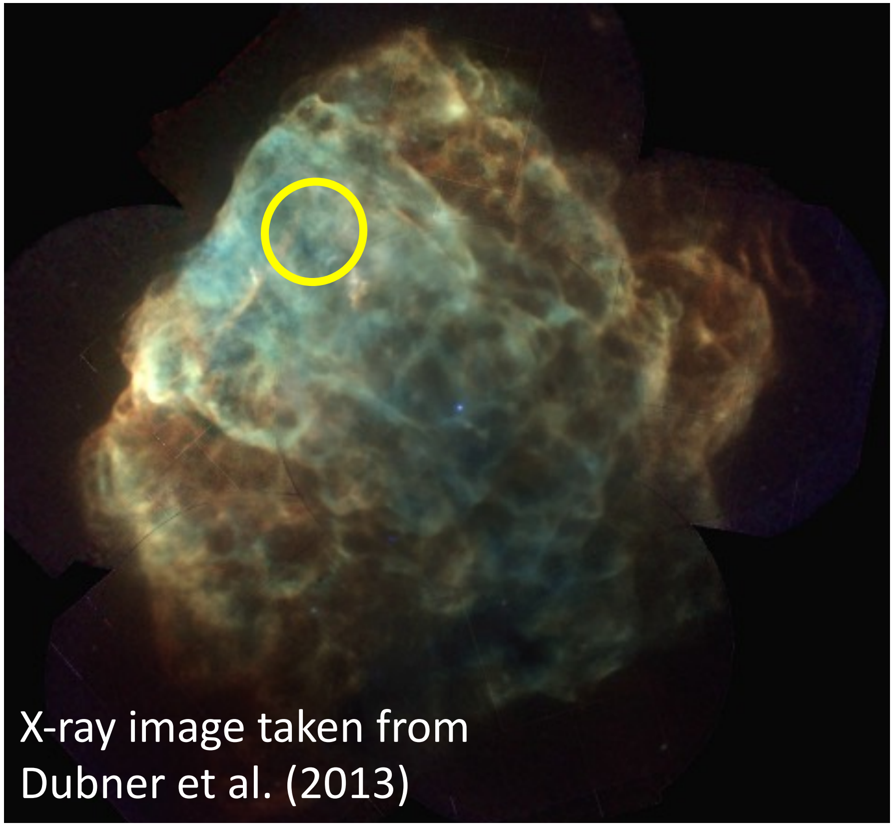

X-ray image taken from Dubner et al. (2013)

Suzaku discovery of Fe K (Mori & Katsuda in prep.)

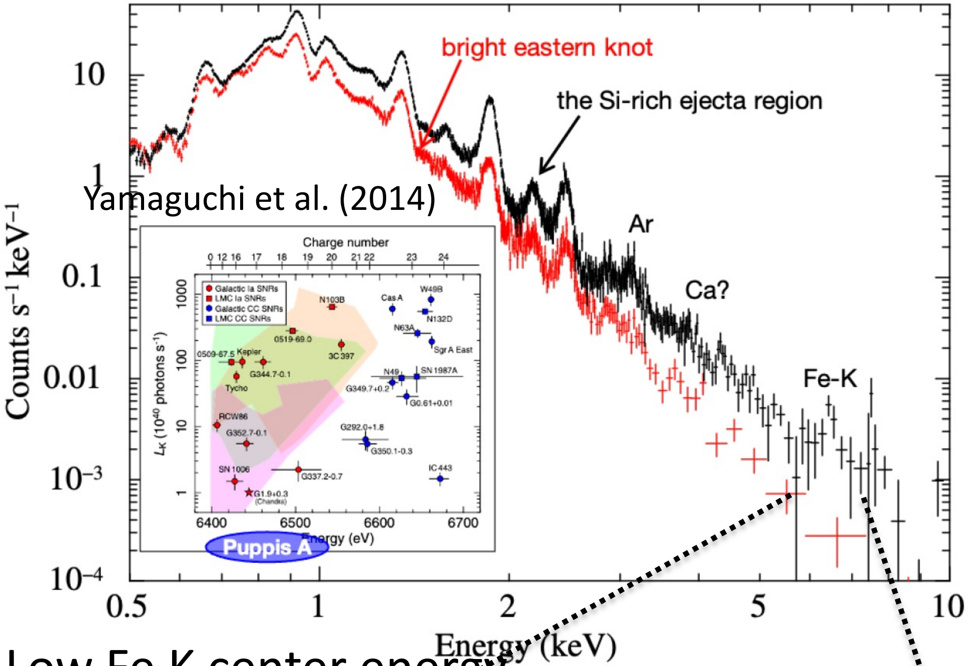

Yamaguchi et al. (2014)

Low Fe K center energy
=> Low-ionization

XRISM simulation with 250 ks

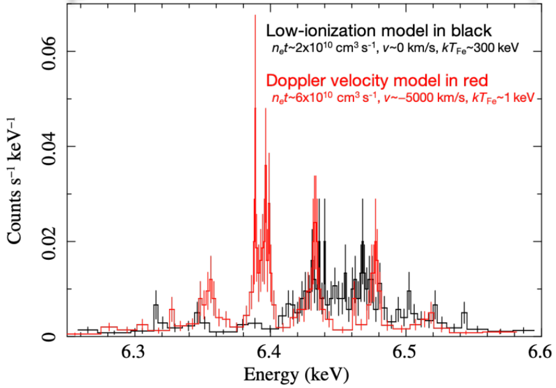

Tycho

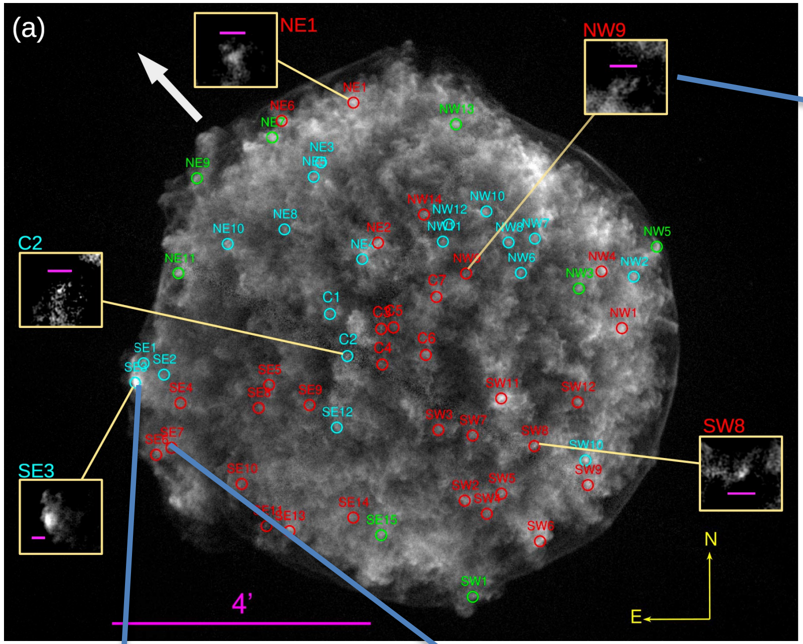

HETG spectroscopy (Millard et al. 2022)

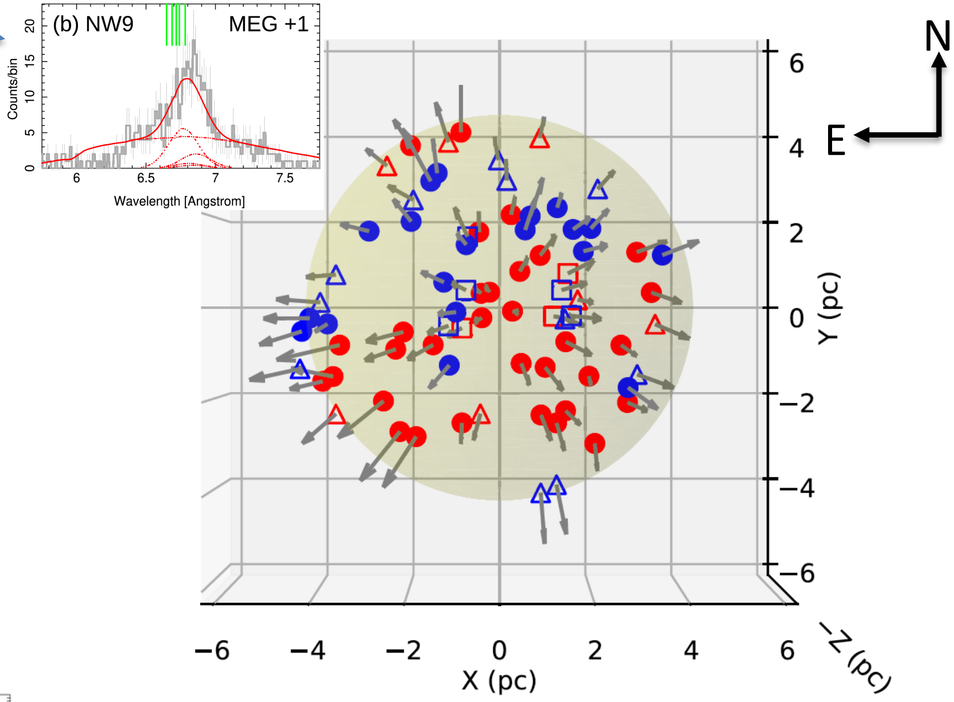

RGS spectroscopy (Williams, SK, et al. 2020)

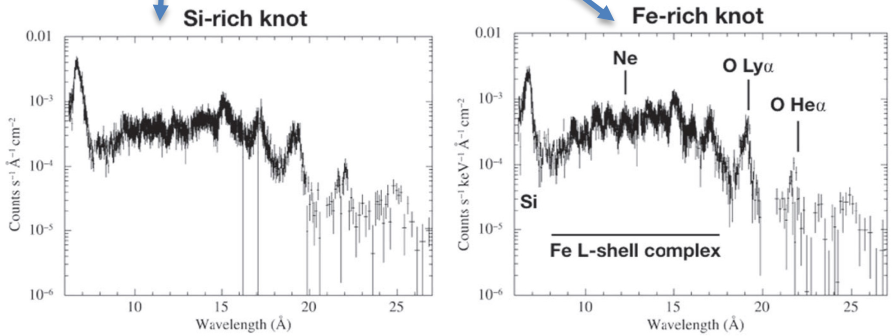

First clear detection of O K lines → relatively rich O

☐ Asymmetric ejecta distribution
N-hemisphere: more blueshift ejecta
S-hemisphere: more redshift ejecta

Kepler: 3D Ejecta Distribution

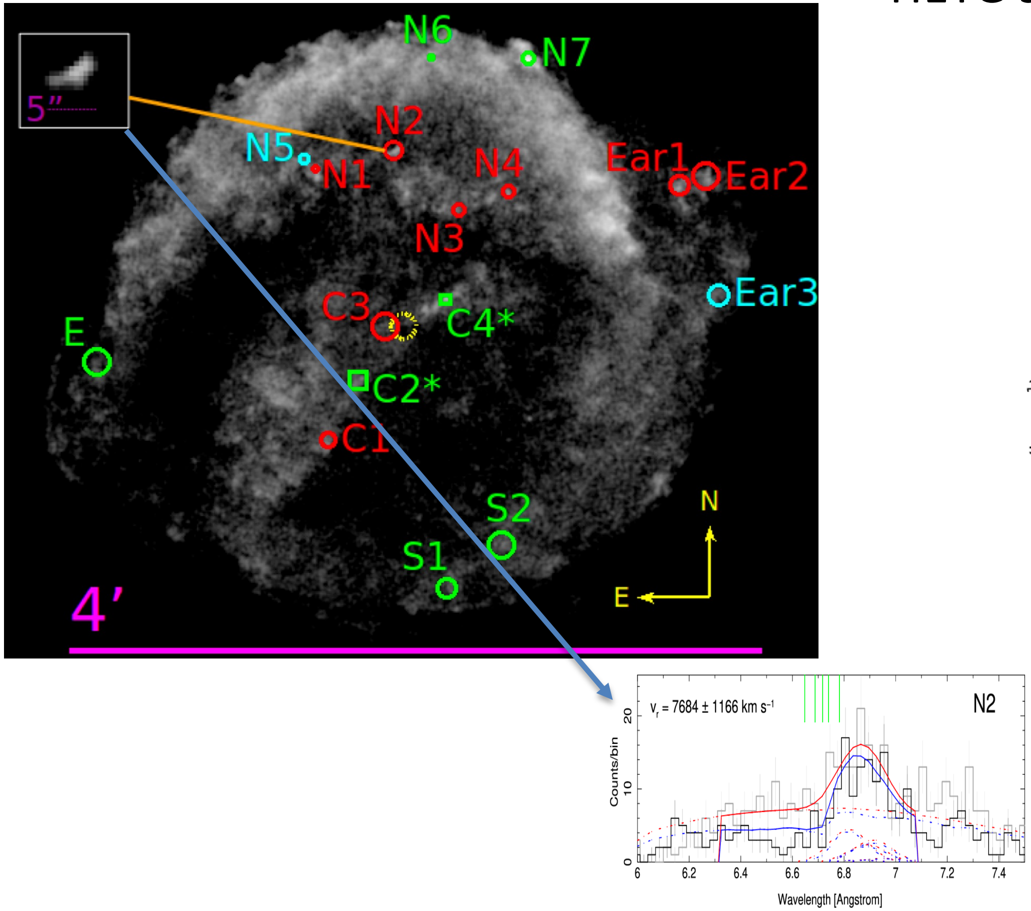

HETG spectroscopy (Millard et al. 2020)

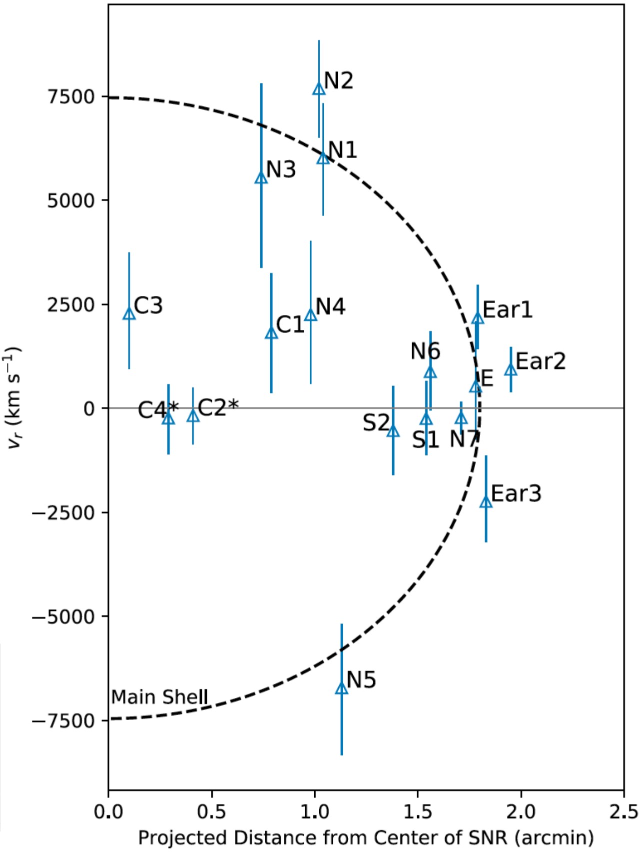

☐ Some ejecta knots are expanding freely (see also, Sato & Hughes 2017).

☐ More ejecta reside in the far side. → Asymmetric explosion? Need more samples.

Kepler: 3D CSM Distribution

RGS spectroscopy (Kasuga, Vink, SK...2021)

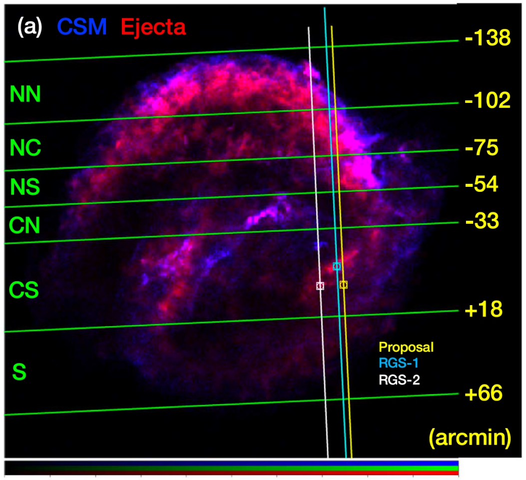

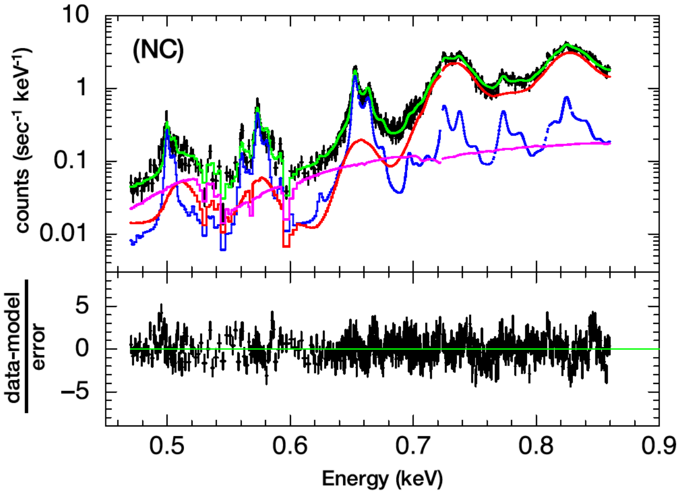

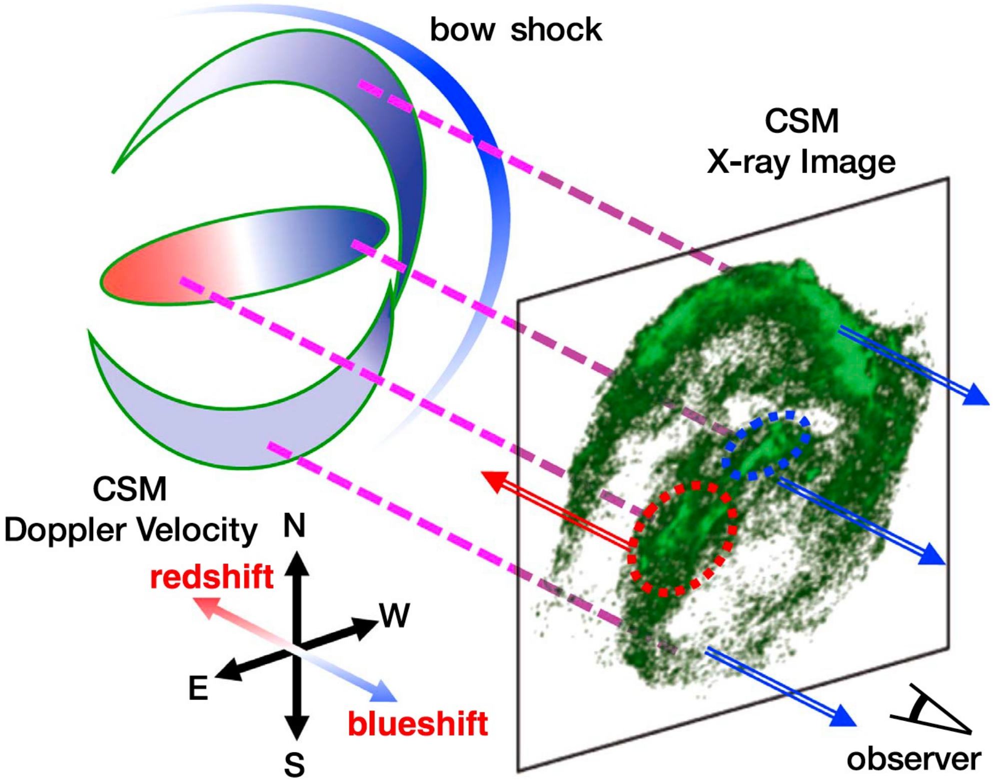

The velocity structure of the CSM is roughly consistent with a runaway progenitor scenario (first proposed by Bandiera 1987).

Geometry of the CSM Ring in SN 1987A

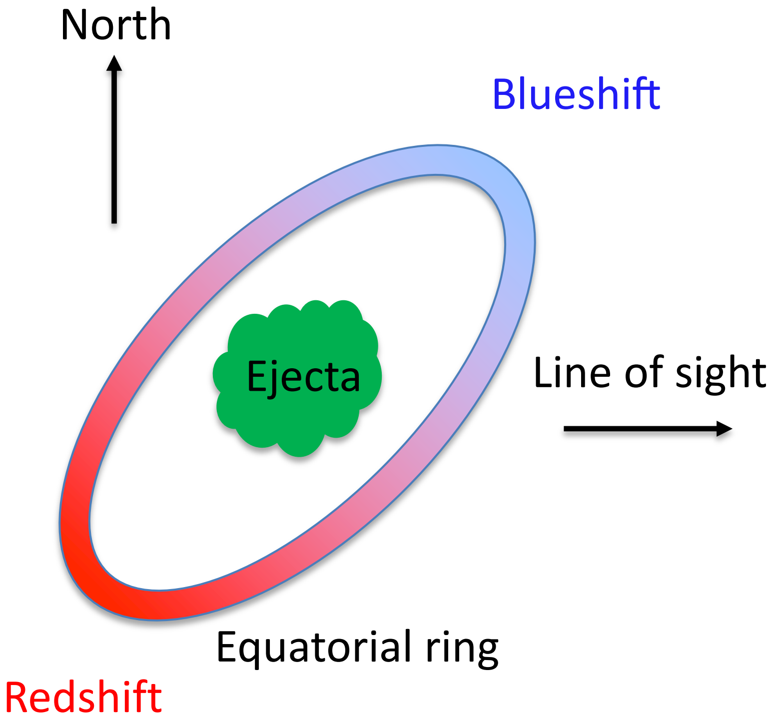

North

Blueshift

Ejecta

Line of sight

Equatorial ring

Redshift

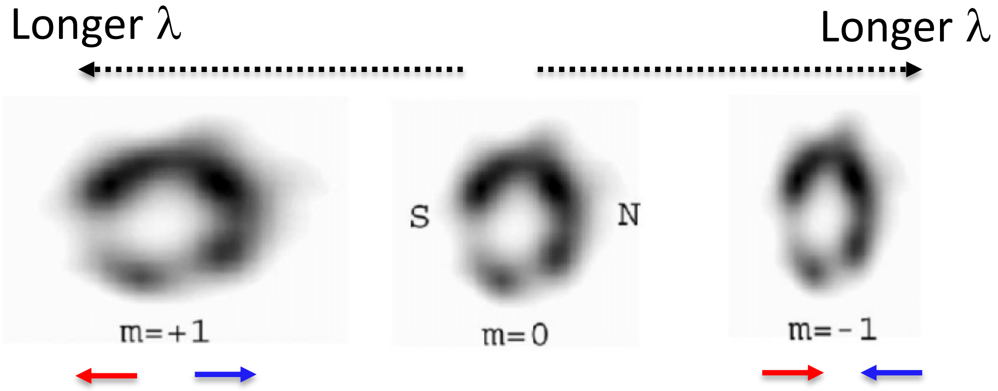

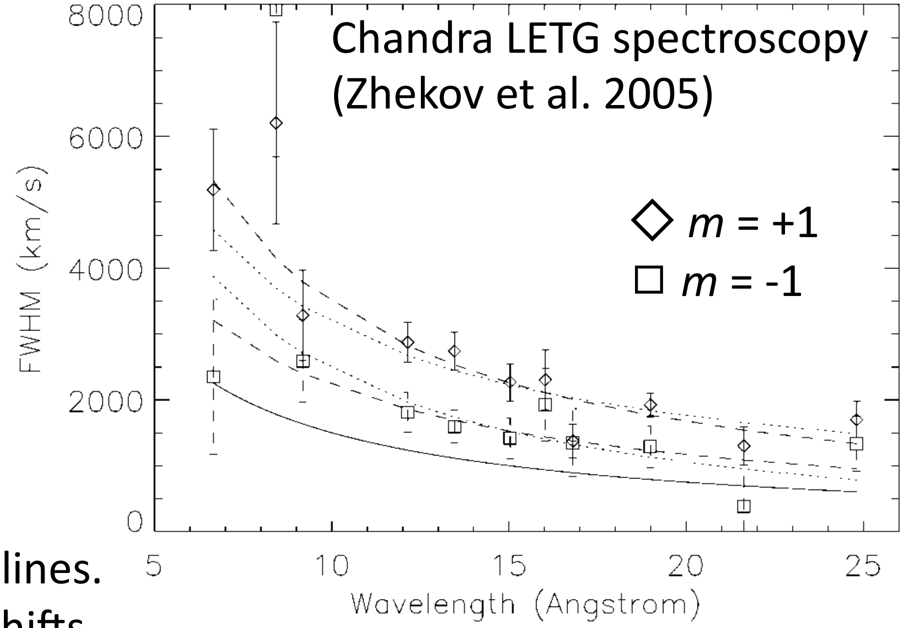

Chandra LETG spectroscopy (Zhekov et al. 2005)

The +1 order lines are broader than -1 order lines.

→ Hints for North-South/Blue-Red Doppler shifts.

A Remarkable Extragalactic Supernovae

HETG spectroscopy (Quirola-Vasquez et al. 2019)

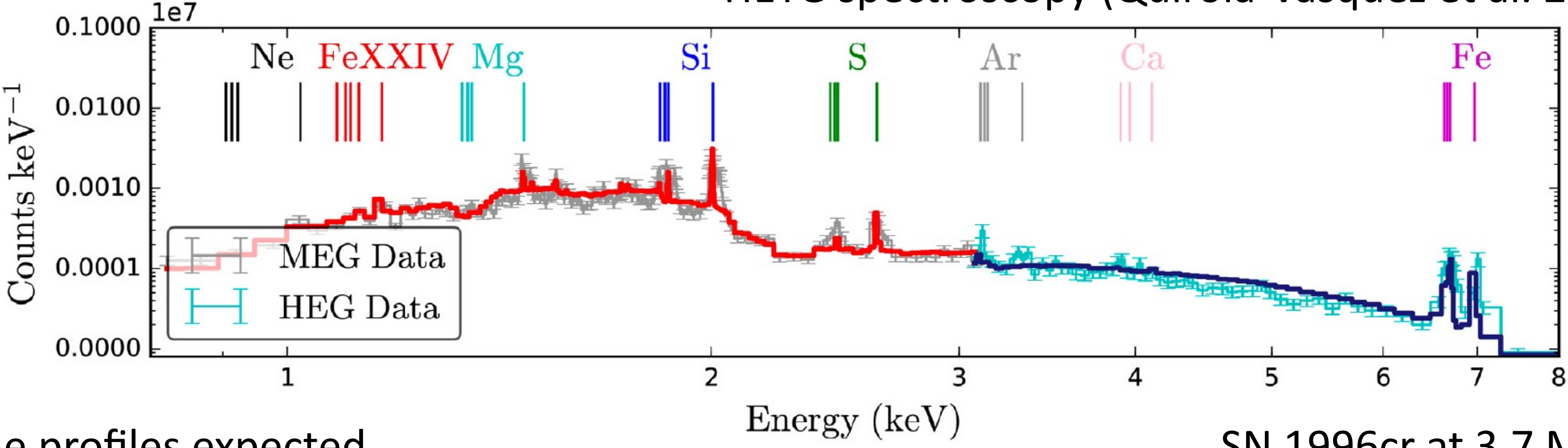

Line profiles expected

SN 1996cr at 3.7 Mpc

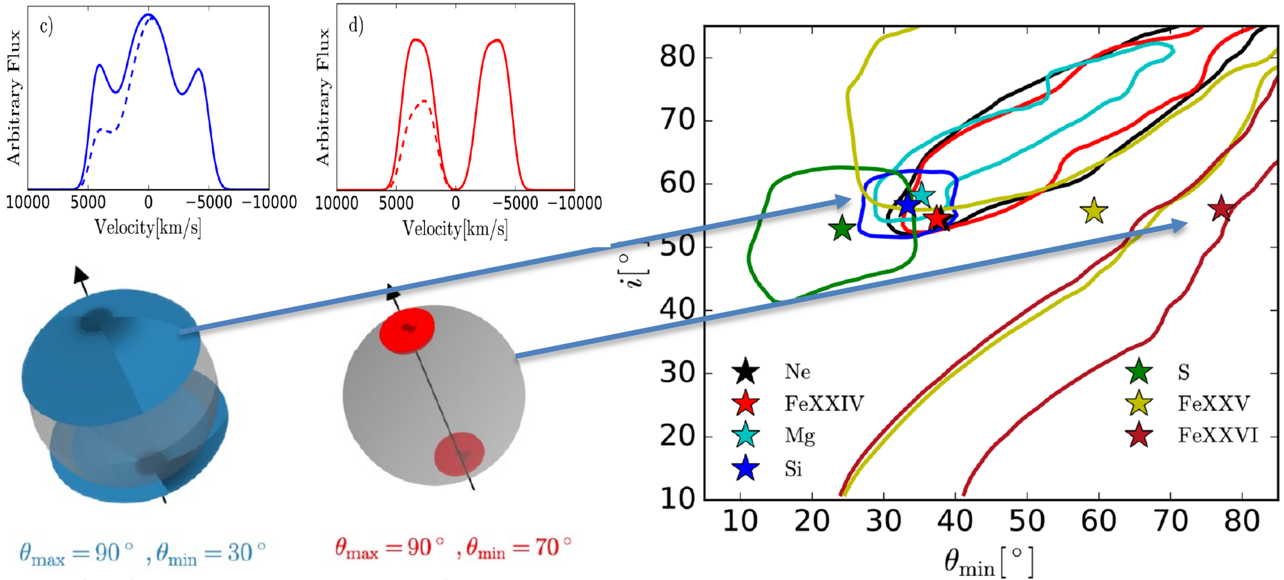

Si ejecta

Fe ejecta

Line profiles can constrain:

- Inclination angle to be ~50°
- Jets' opening angle to be ~20° (Fe); ~60° (Si)

Specific Sciences from High-Res. Spectroscopy

- Ejecta dynamics
  - 3D ejecta structures
    - → Explosion asymmetries & NS kicks
- Collisionless shock physics
  - T_i-T_e equilibration
  - Cosmic-ray acceleration
- Plasma diagnostics
  - Thermodynamic parameters
  - Radiative processes
- Composition measurements
  - Odd-Z/neutron-rich elements

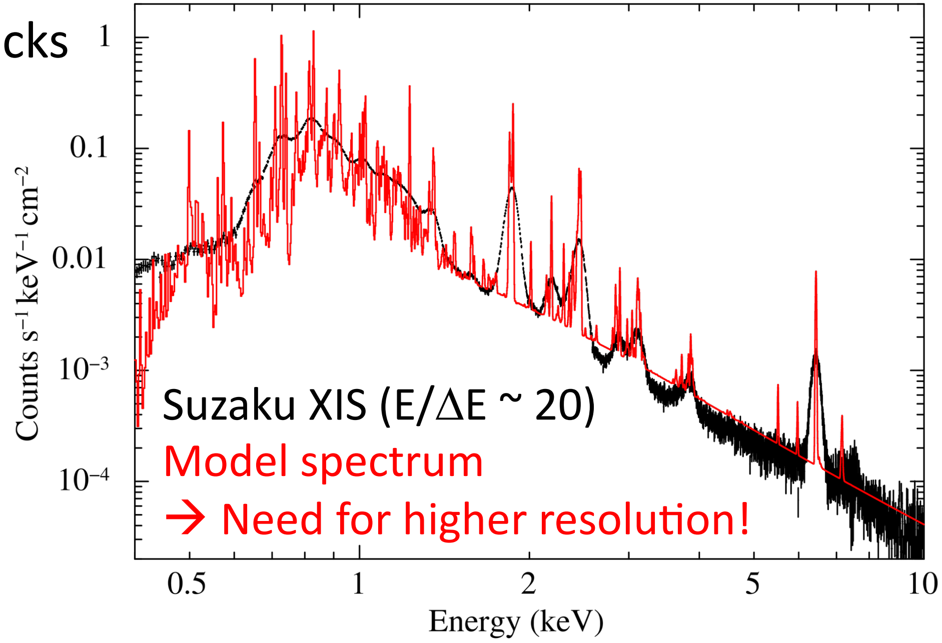

Suzaku XIS (E/ΔE ~ 20)

Model spectrum

→ Need for higher resolution!

SN 1006: Temperature Nonequilibration ($T_O >> T_e$)

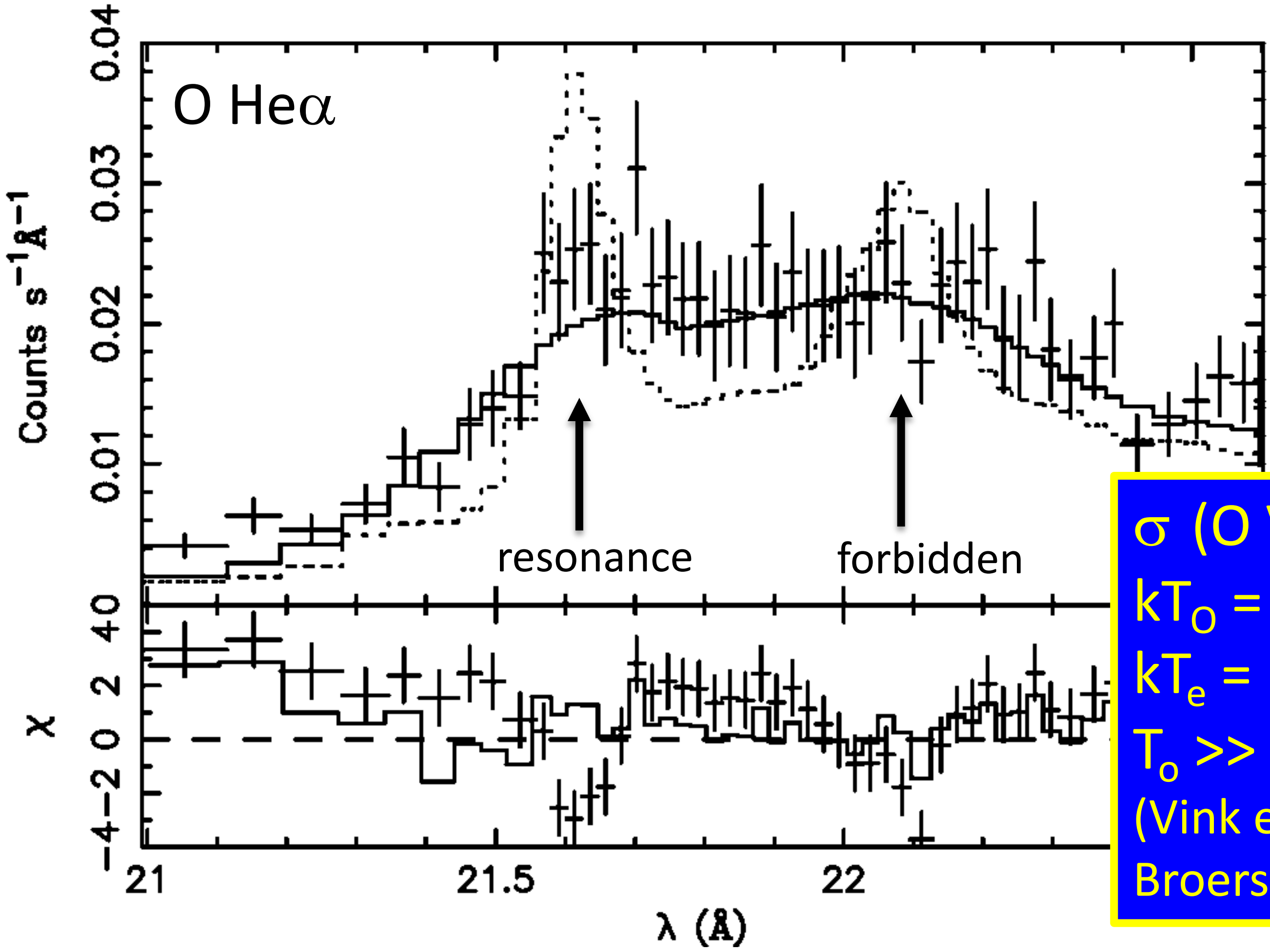

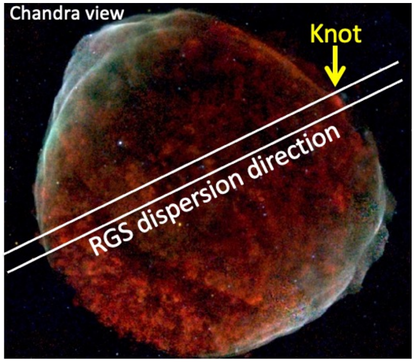

σ (O VII) = 3.4 ± 0.5 eV

kT_O = 530 ± 150 keV

kT_e = 1.5 keV

$T_o >> T_e$!

(Vink et al. 2003; see also Broersen et al. 2013)

Dotted line: emission model w/o thermal broadening

Solid line: emission model w/ thermal broadening

$$\sigma = E_0\sqrt{kT/mc^2}$$

Tycho: Temperature Nonequilibration ($T_i >> T_e$)

Williams, SK+ (2020)

Global fit with the data requires line broadening of ~5 eV at 1 keV.
If the broadening is totally thermal Doppler effects:
kT_O ~ 400 keV & kT_{Fe} ~ 1.4 MeV

$$\sigma = E_0\sqrt{kT/mc^2}$$

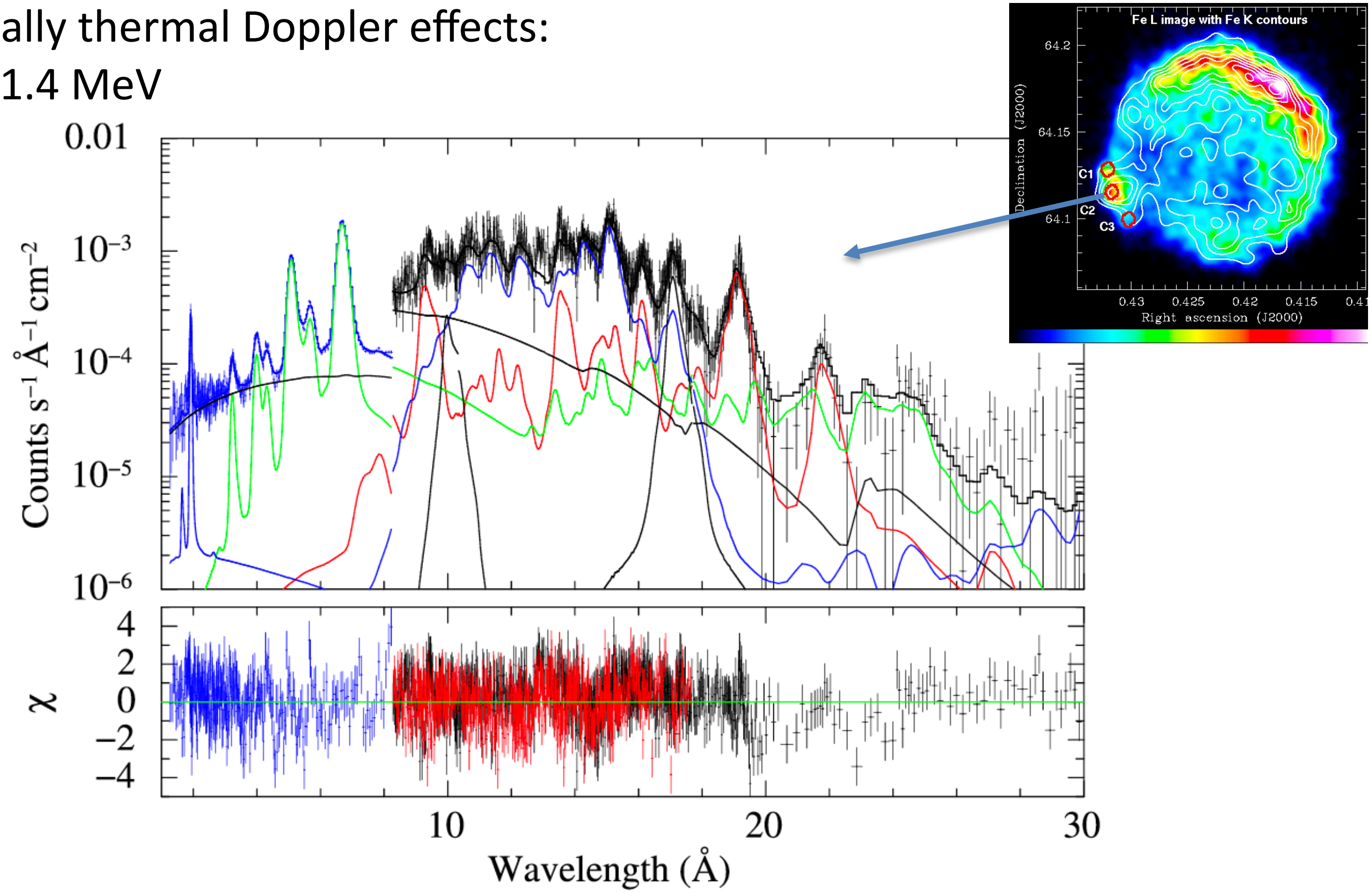

The (reverse) shock speed is estimated to be 3500 km/s.

SN 1987A: Temperature Nonequilibration ($T_i >> T_e$)

HETG spectroscopy (Miceli et al. 2019)

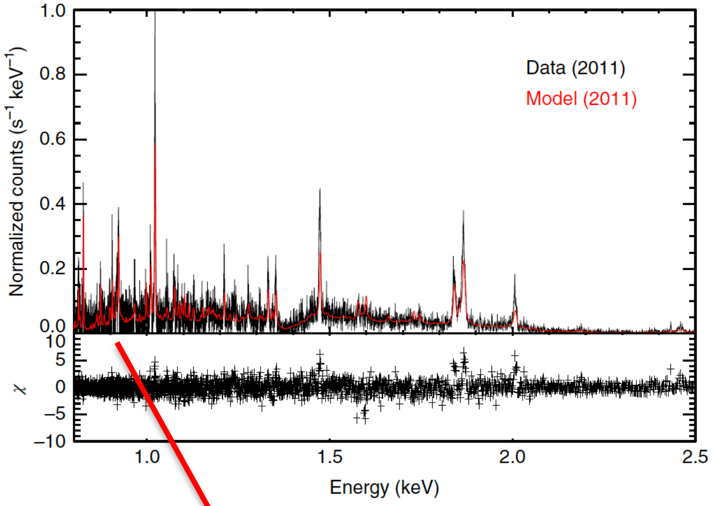

Comparison with a hydrodynamic model revealed thermal broadening.

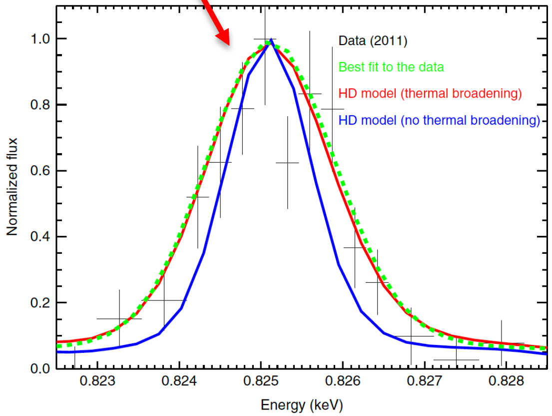

The ion temperatures are in good agreement with the mass-proportional temperature.

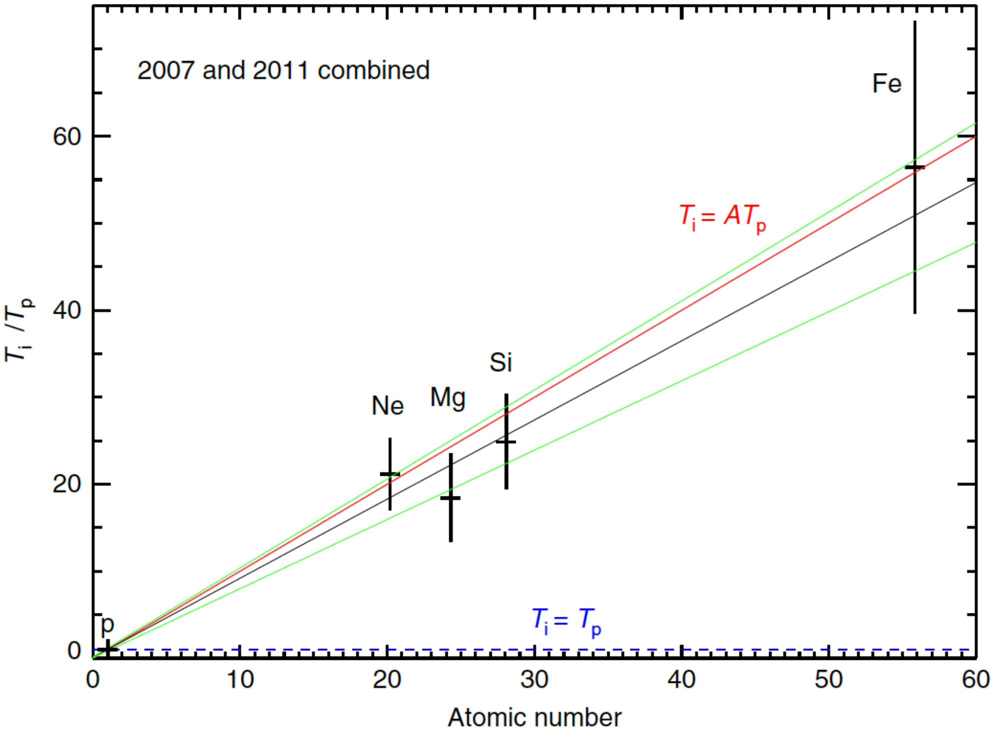

Specific Sciences from High-Res. Spectroscopy

- Ejecta dynamics
  - 3D ejecta structures
- Collisionless shock physics
  - T_i-T_e equilibration
  - Cosmic-ray acceleration
- Plasma diagnostics
  - Thermodynamic parameters
  - New radiative processes
- Composition measurements
  - Odd-Z/neutron-rich elements

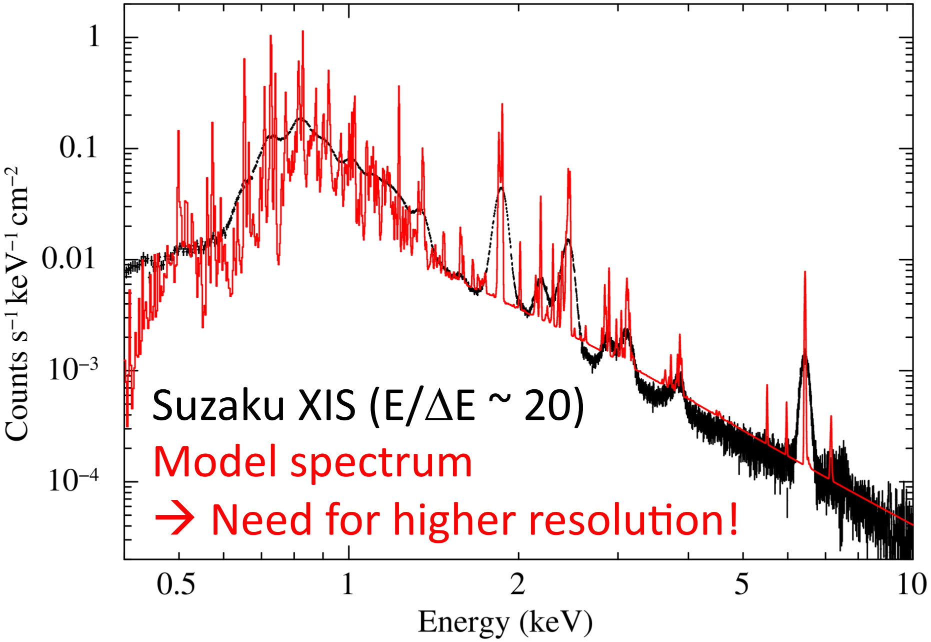

Suzaku XIS (E/ΔE ~ 20)

Model spectrum

→ Need for higher resolution!

Anomalously High O VII Heα f/r Ratios

RGS spectra revealed that O VII Heα f/r ratios are higher than expected in some SNRs.

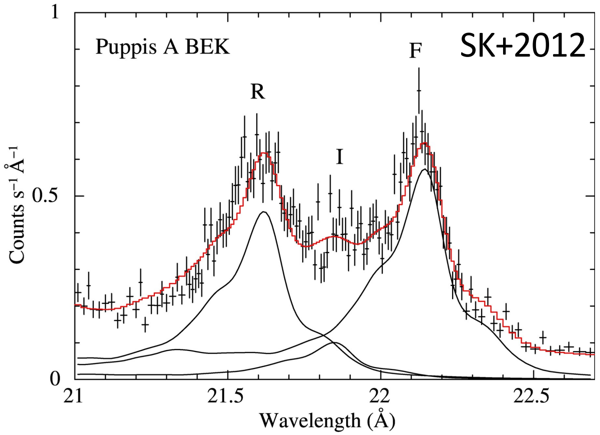

G296.1-0.5

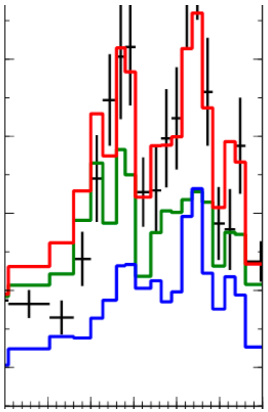

Tanaka+2022

N132D

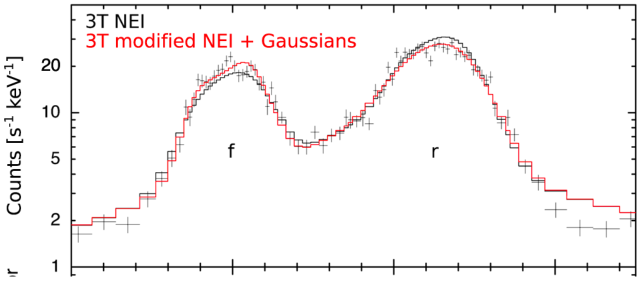

Suzuki+2020

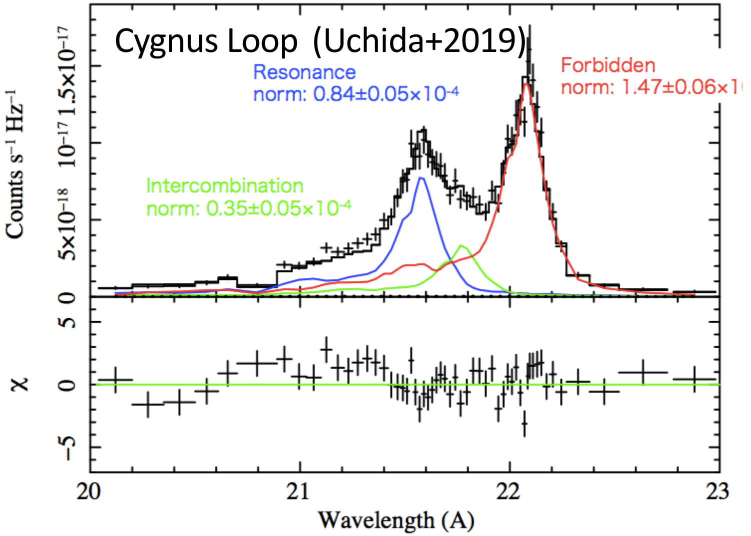

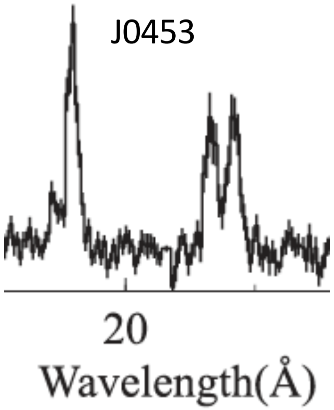

Koshiba+2022

N49

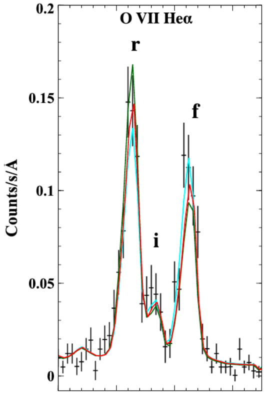

Amano+2020

Possible Causes of Anomalous f/r Ratios

- Reducing “r” line
  - Resonance scattering (self absorption)
  - Absorption by foreground ionized ISM
- Enhancing “f” line
  - Charge exchange
  - Recombination (recombination-dominated plasmas)
  - Inner-shell ionization (low-T and/or low-nt plasmas)
  - Proton excitation (resonance line is absent)

Recent Interesting Finding from N132D

Strong high-n transition lines may be a signature of CX X-rays.

Resolve spectrum from the entire remnant

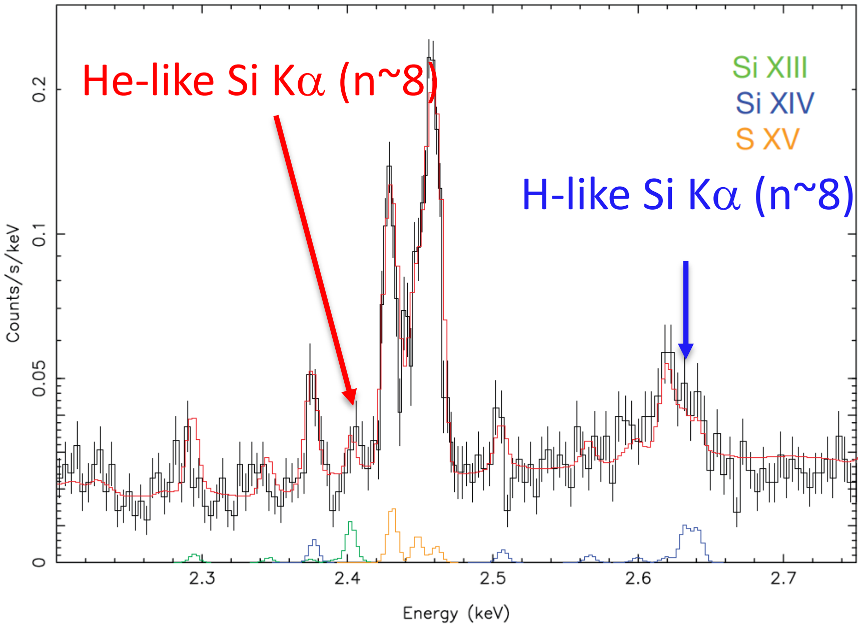

RGS1 1st order from the north rim

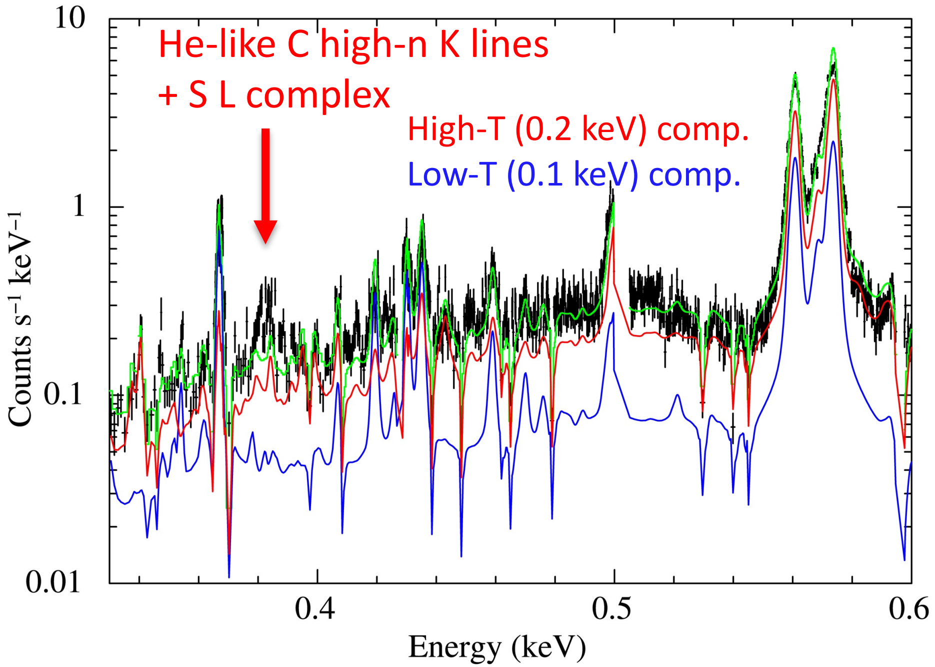

XRISM collaboration to be submitted to PASJ
Presented by Brian Williams
(See also, XRISM first light press release: https://www.jaxa.jp/press/2024/01/20240105-1_j.html)

SK et al. in prep.

Specific Sciences from High-Res. Spectroscopy

- Ejecta dynamics
  - 3D ejecta structures
- Collisionless shock physics
  - T_i-T_e equilibration
  - Cosmic-ray acceleration
- Plasma diagnostics
  - Thermodynamic parameters
  - New radiative processes
- Composition measurements
  - Odd-Z/neutron-rich elements

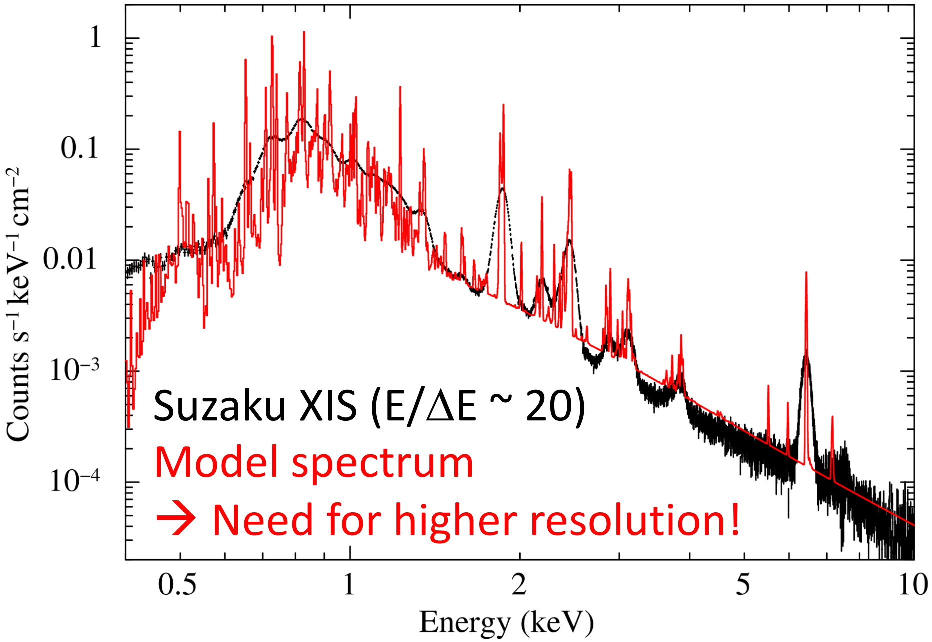

Suzaku XIS (E/ΔE ~ 20)

Model spectrum

→ Need for higher resolution!

CNO Abundances of the CSM in SNRs

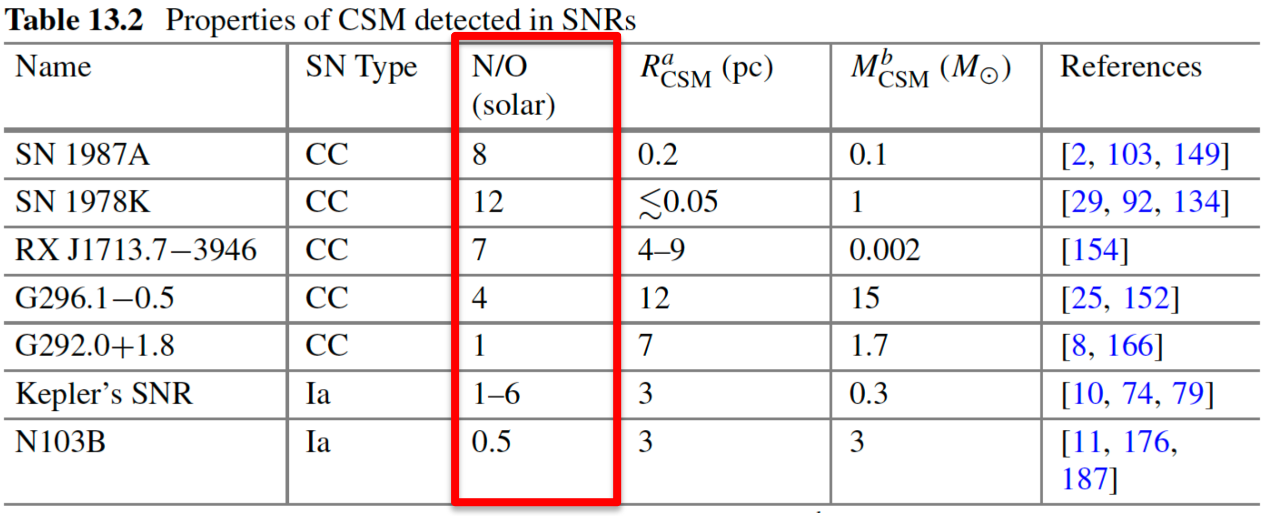

Table 13.2 Properties of CSM detected in SNRs

Name	SN Type	N/O (solar)	$R^a_{\rm CSM}$ (pc)	$M^b_{\rm CSM}$ ($M_\odot$)	References
SN 1987A	CC	8	0.2	0.1	[2, 103, 149]
SN 1978K	CC	12	$\lesssim$0.05	1	[29, 92, 134]
RX J1713.7−3946	CC	7	4–9	0.002	[154]
G296.1−0.5	CC	4	12	15	[25, 152]
G292.0+1.8	CC	1	7	1.7	[8, 166]
Kepler's SNR	Ia	1–6	3	0.3	[10, 74, 79]
N103B	Ia	0.5	3	3	[11, 176, 187]

Table from SK (2023)

RGS spectroscopy of a CSM knot in RX J1713 (Tateishi, SK+ 2021).

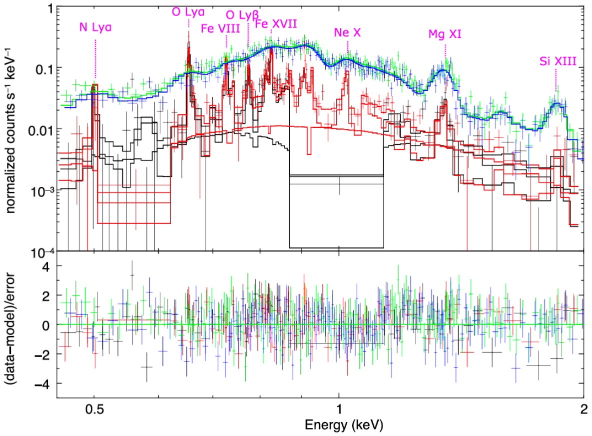

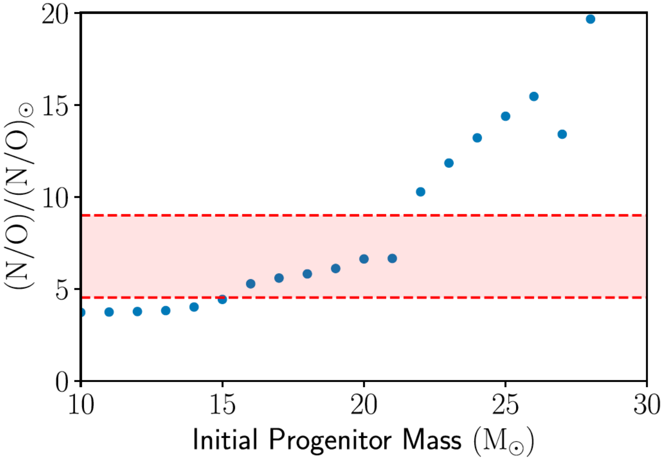

The N/O abundance ratio in the stellar wind is more enhanced with increasing $M_{\rm ZAMS}$, as dM/dt increases with $M_{\rm ZAMS}$.

=> N/O can constrain $M_{\rm ZAMS}$.

More Recent Progresses in CNO Studies

RCW 103

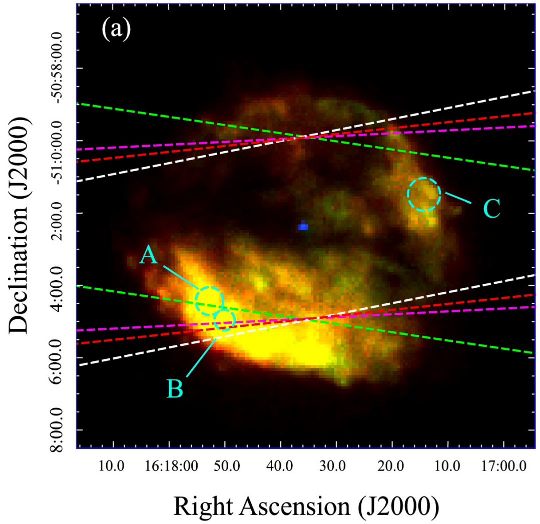

RGS spectroscopy (Narita et al. 2023)

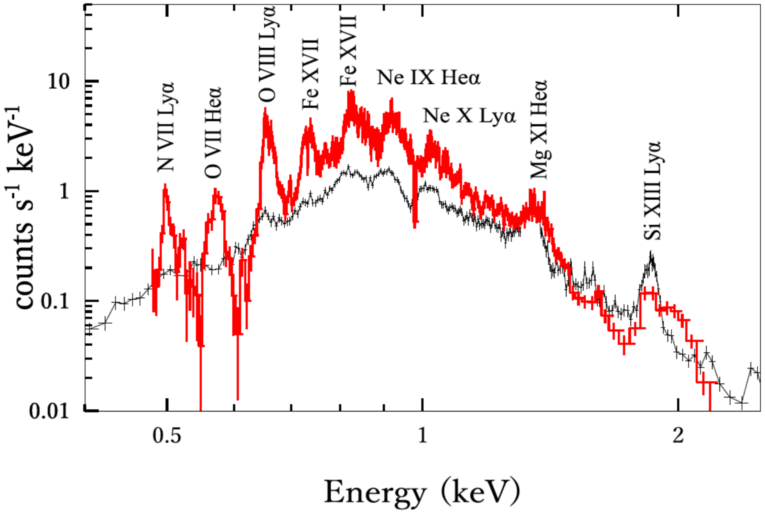

N/O = 3.8±0.1 solar

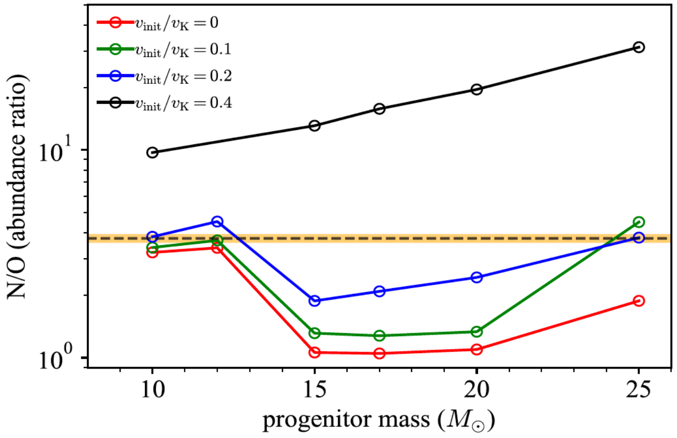

In this case, a low-mass (10-12 $M_\odot$), relatively slow rotation (<100 km/s) progenitor is preferred.
CNO abundance is essential to determine the progenitor mass, rotation, and evolution, and overshoot parameters (e.g., Uchida & Narita 2023).

See also Posters S3-23 & S3-2 by Narita et al. and Anazawa et al.

Micro-calorimeter (Resolve) aboard XRISM

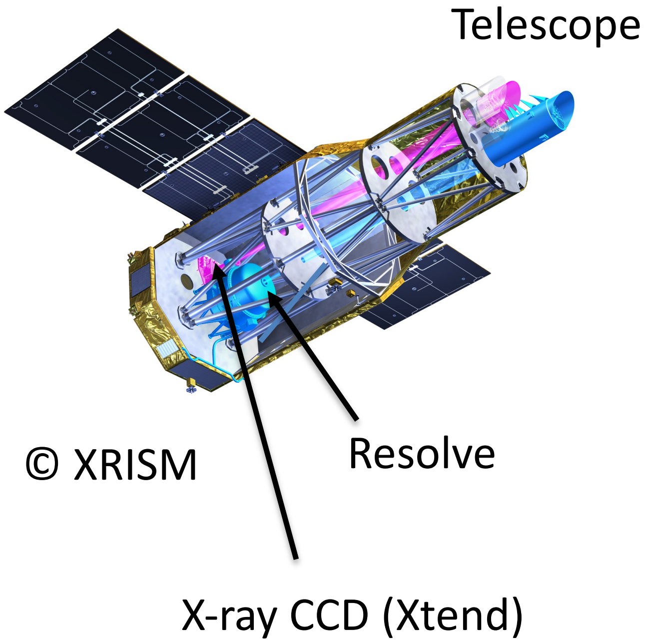

© XRISM

☐ XRISM:

- The 7th Japanese X-ray astronomy satellite
- Successfully launched on Sep. 7th 2023

☐ SNRs (to be) observed in the Performance Verification phase:

N132D*, Cas A*, Tycho, Sgr-A East, Kepler, W49B, 3C397, SN 1987A, SN 2024iss, Cygnus Loop (cal), E0102 (cal)

*Talks by Brian Williams and Paul Plucinsky

XRISM will deliver many exciting results shortly!

However, the energy coverage is currently limited to 2-10 keV. Therefore, gratings aboard XMM and Chandra are still very important to fully explore X-ray emission.

Chapter 13 of the Springer Book “High-resolution X-ray spectroscopy”

arXiv:2302.13775

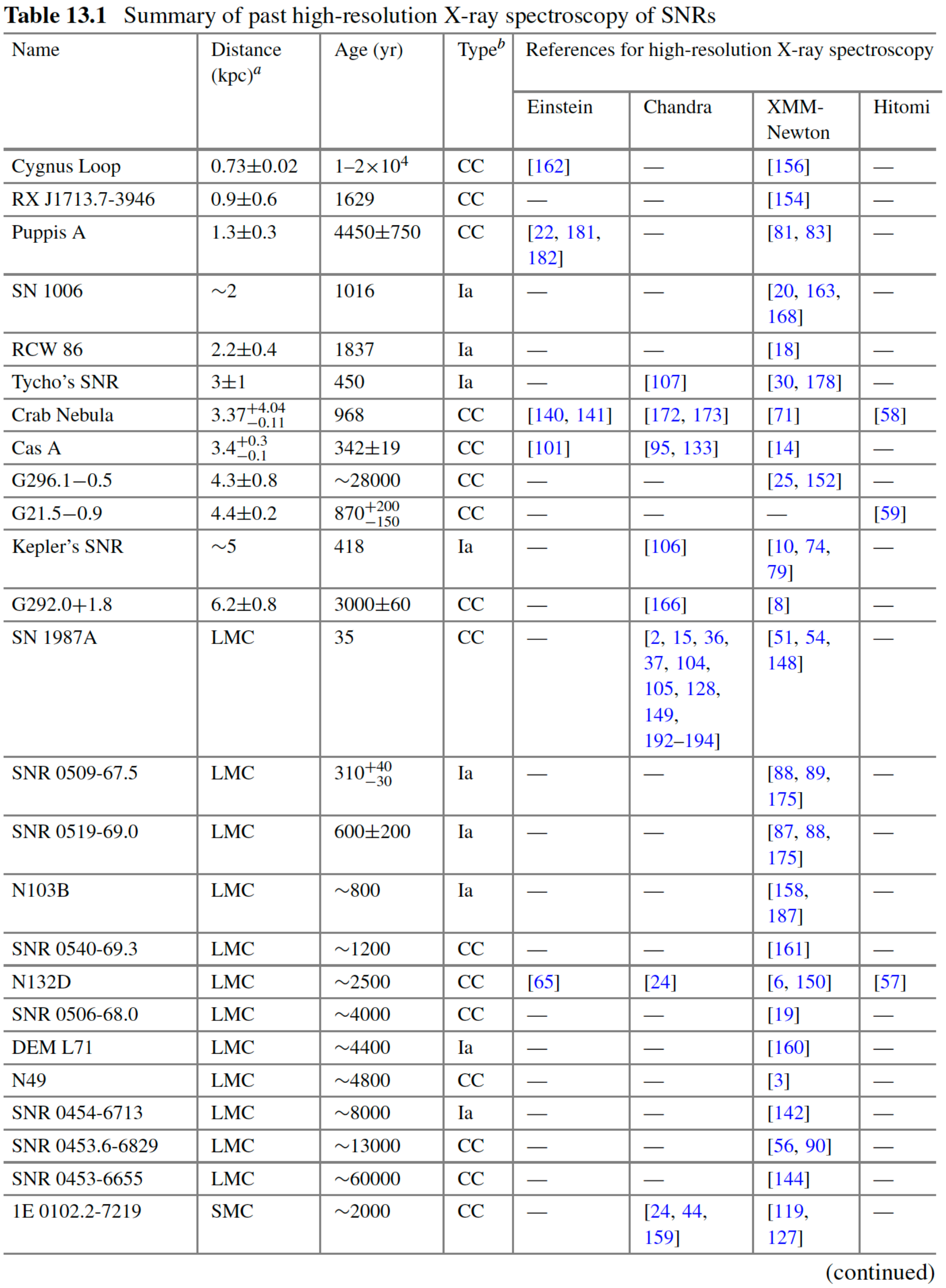

Table 13.1 Summary of past high-resolution X-ray spectroscopy of SNRs

Name	Distance (kpc)^a	Age (yr)	Type^b	References for high-resolution X-ray spectroscopy			
				Einstein	Chandra	XMM-Newton	Hitomi
Cygnus Loop	0.73±0.02	$1–2\times10^4$	CC	[162]	—	[156]	—
RX J1713.7-3946	0.9±0.6	1629	CC	—	—	[154]	—
Puppis A	1.3±0.3	4450±750	CC	[22, 181, 182]	—	[81, 83]	—
SN 1006	∼2	1016	Ia	—	—	[20, 163, 168]	—
RCW 86	2.2±0.4	1837	Ia	—	—	[18]	—
Tycho’s SNR	3±1	450	Ia	—	[107]	[30, 178]	—
Crab Nebula	$3.37^{+4.04}_{-0.11}$	968	CC	[140, 141]	[172, 173]	[71]	[58]
Cas A	$3.4^{+0.3}_{-0.1}$	342±19	CC	[101]	[95, 133]	[14]	—
G296.1−0.5	4.3±0.8	∼28000	CC	—	—	[25, 152]	—
G21.5−0.9	4.4±0.2	870^{+200}_{-150}	CC	—	—	—	[59]
Kepler’s SNR	∼5	418	Ia	—	[106]	[10, 74, 79]	—
G292.0+1.8	6.2±0.8	3000±60	CC	—	[166]	[8]	—
SN 1987A	LMC	35	CC	—	[2, 15, 36, 37, 104, 105, 128, 149, 192–194]	[51, 54, 148]	—
SNR 0509-67.5	LMC	310^{+40}_{-30}	Ia	—	—	[88, 89, 175]	—
SNR 0519-69.0	LMC	600±200	Ia	—	—	[87, 88, 175]	—
N103B	LMC	∼800	Ia	—	—	[158, 187]	—
SNR 0540-69.3	LMC	∼1200	CC	—	—	[161]	—
N132D	LMC	∼2500	CC	[65]	[24]	[6, 150]	[57]
SNR 0506-68.0	LMC	∼4000	CC	—	—	[19]	—
DEM L71	LMC	∼4400	Ia	—	—	[160]	—
N49	LMC	∼4800	CC	—	—	[3]	—
SNR 0454-6713	LMC	∼8000	Ia	—	—	[142]	—
SNR 0453.6-6829	LMC	∼13000	CC	—	—	[56, 90]	—
SNR 0453-6655	LMC	∼60000	CC	—	—	[144]	—
1E 0102.2-7219	SMC	∼2000	CC	—	[24, 44, 159]	[119, 127]	—

(continued)

Summary

- High-resolution X-ray spectroscopy is a long-anticipated discovery space especially for diffuse sources like SNRs.
- Cutting-edge researches have been explored by grating spectrometers onboard XMM-Newton and Chandra.
- The Japan-US X-ray astronomy satellite, XRISM (2023-), is now vigorously developing this research field.